Preprints of the 18th IFAC World Congress
Milano (Italy) August 28 - September 2, 2011

# Active-Passive Decentralized $H_\infty$ Control for Adjacent Buildings Under Seismic Excitation

**F. Palacios-Quiñonero** *, **J.M. Rossell** *, **J. Rodellar** **, and **H.R. Karimi** ***

* *Dept. of Applied Mathematics III, Universitat Politècnica de Catalunya (UPC), Campus Manresa, 08242-Manresa (Barcelona), Spain. (francisco.palacios@upc.edu), (josep.maria.rossell@upc.edu)*
** *Dept. of Applied Mathematics III, Universitat Politècnica de Catalunya (UPC), Campus Nord, C2, 08034-Barcelona, Spain. (jose.rodellar@upc.edu)*
*** *Dept. of Engineering, University of Adger, Norway (hamid.r.karimi@uia.no)*

Abstract: In this paper, a control strategy to reduce the vibrational response of adjacent buildings under seismic excitation is presented. The proposed strategy combines passive linking elements with an active decentralized $H_\infty$ control system. The overall active-passive control system admits decentralized design and operation, and achieves an excellent vibrational reduction when the active control system works; in case of a full or partial failure of the active control system, a remarkable reduction in the vibrational response is guaranteed by the passive linking elements. For adjacent buildings that require different levels of seismic protection, the implementation of an active $H_\infty$ control system in just one of the buildings is also considered. The main ideas are presented by means of a simplified two-building model. Numerical simulations have been carried out to assess the performance of the proposed methodology with promising results.

*Keywords:* Decentralized control, H-infinity control, structural vibration control, linear matrix inequalities.

## 1. INTRODUCTION

Over the last decades, Structural Vibration Control (SVC) for seismic hazard mitigation has become an active research field. Significant advances, both theoretical and experimental, have been made in protecting buildings and civil structures from the destructive effects of seismic events. Different kinds of energy dissipation devices and control strategies have been developed and tested with positive results, both at simulation level and in full-scale implementations. Attending to external energy requirements, SVC systems are commonly classified in three broad categories: passive, active, and semi-active systems. Passive SVC systems do not require an external power source, they are simple, compact, reliable, and may achieve remarkable but limited results. Active SVC systems can be more effective; however, they require a large external power supply, massive and complex actuation devices, accurate state information, and may produce instability. Finally, recently developed semi-active SVC systems can operate on battery power and combine the simplicity and reliability of passive systems with the performance levels and flexibility of full active systems. In this case, one of the main difficulties is the nonlinear nature of semiactive devices, which makes the design of feedback control strategies a challenging task. A good survey can be found in Housner et al. (1997), and Spencer and Nagarajaiah (2003).

Although the most appealing examples of SVC implementations are those involving huge structures as high towers or long-span bridges, it should be noted the existence of a large variety of medium-size and small-size strategic structures for which seismic protection may be of critical importance. Some clear examples are communication and command centers, emergency service facilities, hospitals, emergency power plants, etc. In all these cases, it is not enough to prevent structural failure and ensure safety, but also operational serviceability of the structure and equipment needs to be assured. Moreover, despite the medium or small size of individual buildings, the overall structure may be highly complex comprising two or more adjacent buildings and a variety of attached substructures, possibly requiring different levels of seismic protection.

When dealing with the seismic response of closely adjacent structures, the possibility of inter-structure collisions (pounding) should be considered. Pounding may cause severe structural damage, even collapse in some extreme situations Anagnostopoulos (1996). Further, large acceleration pulses may result from the quick and massive pound-

[1] This work was supported in part by the Spanish Ministry of Science and Innovation and FEDER funds from the European Union through the Grants DPI2008-06699 and DPI2008-06564-C02-02

ing impacts, which can cause serious damage to building contents Lopez-Garcia and Soong (2009). It is also worth to be noted that some seismic protection strategies such as passive base isolation, which can effectively reduce the seismic response of isolated buildings, may also increase the risk of pounding between insufficiently spaced adjacent structures Matsagar and Jangid (2005).

In recent years, the Connected Control Method (CCM) has proved to be an effective strategy to simultaneously mitigate pounding effects and achieve vibrational response reduction. In the CCM, closely adjacent structures are linked together by coupling devices to provide appropriate reaction control forces. The application of the CCM using different kinds of passive, active, and semiactive linking devices have been investigated with positive results. Two recent and interesting references are Bharti et al. (2010) and Preumont and Seto (2008).

The aim of this work is to explore the seismic response of a complex structure consisting of two adjacent actively controlled buildings linked by damping passive elements. The resulting active-passive overall control system combines the high performance characteristics of active control systems with the reliability of passive control elements and, at the same time, admits a decentralized design and operation of the active control subsystems. More precisely, we consider a two-building coupled system with the following control structure (see Fig. 1): (i) Every story is equipped with an ideal active actuator, (ii) passive energy dissipation devices are located at the linking elements, (iii) in each building, the active actuators are operated by an independent feedback local controller.

The seismic response of the two-building system when the decentralized active control system is partially or totally switched off is a particularly relevant subject, which admits two interesting practical interpretations: from a reliability point of view, it can be seen as the system response under a partial or full failure of the active control system; from a design point of view, it can be understood as the response produced by different active control configurations corresponding to different levels of seismic protection.

Due to the complexity of the overall system, we have chosen a minimal configuration that allows a clear presentation of the main ideas while maintaining the generality of the approach. This configuration consists of a three-story building linked to a two-story building. The linking passive elements have been modeled as viscoelastic dampers. For the overall system, a state feedback centralized $H_\infty$ controller has been obtained, which have been taken as a reference in the performance assessment. The design of the decentralized controller has been carried out following two different strategies. First, a decentralized $H_\infty$ controller has been obtained using the whole model of the coupled two-building system by imposing suitable structure constraints in the corresponding LMIs. Second, $H_\infty$ controllers have been independently computed for each building ignoring the passive linking.

Numerical simulations of the vibrational response of the two-building system have been conducted, using the El Centro NS 1940 earthquake as ground acceleration. The simulation data indicate that, despite the decentralized design and the restricted information exchange, the results obtained by the decentralized active controllers are similar to those attained by the centralized active controller. When the decentralized active control system is completely switched off, a remarkable reduction of the maximum inter-story drifts in both buildings is guaranteed by the passive elements. If only one of the local active controllers is disabled, the response of the actively controlled building remains practically unaffected; moreover, the control forces in the working active devices increase slightly and act through the linking elements to drive the response of the uncontrolled building to a level that is clearly below the level obtained by the pure passive control.

The paper is organized as follows. In Section 2, a simplified model of the two-building coupled system is provided. In Section 3, two different decentralized controllers together with a centralized controller, which serves as reference, are computed. A brief summary relative to $H_\infty$ control is also included. Finally, in Section 4, numerical simulations of the free and controlled responses for the different cases under consideration are presented and compared.

## 2. TWO-BUILDING MODEL

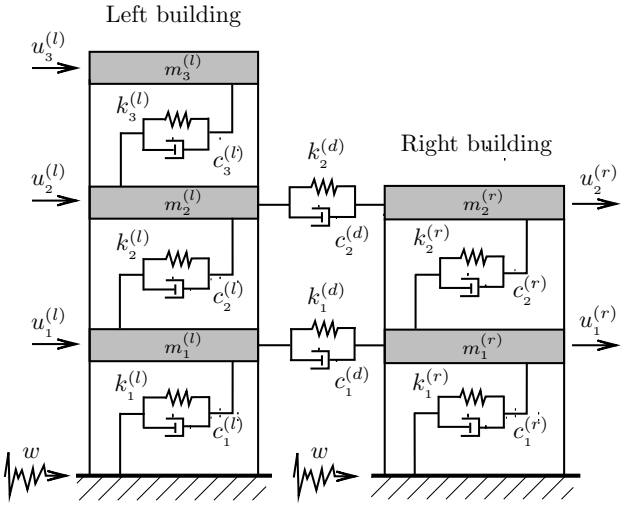


Figure 1. Structural model for two adjacent buildings

In this section, a simplified model for a two-building coupled system formed by a three-story building and a two-story building linked by viscoelastic dampers is presented. The buildings motion can be described by

$$\mathbf{M}\,\ddot{q}(t) + \mathbf{C}\,\dot{q}(t) + \mathbf{K}\,q(t) = \mathbf{T_u}\,u(t) - \mathbf{M}\,\mathbf{T_w}\,w(t), \quad (1)$$

where $\mathbf{M}$ is the mass matrix; $\mathbf{K}$ and $\mathbf{C}$ are the total stiffness and damping matrices, respectively, including the stiffness and damping coefficients of the buildings as well as the stiffness and damping coefficients of the viscoelastic dampers; the vector of relative displacements with respect to the ground is

$$q(t) = \left[q_1^{(l)}(t), q_2^{(l)}(t), q_3^{(l)}(t), q_1^{(r)}(t), q_2^{(r)}(t)\right]^T,$$

where $q_i^{(l)}(t)$ and $q_i^{(r)}(t)$ represent, respectively, the displacement of the $i$th story in the left and right building; the vector of control forces has a similar structure

$$u(t) = \left[u_1^{(l)}(t), u_2^{(l)}(t), u_3^{(l)}(t), u_1^{(r)}(t), u_2^{(r)}(t)\right]^T;$$

$\mathbf{T_u}$=$\mathbf{I}_{5\times5}$ is the control location matrix; $\mathbf{T_w}$ is the index vector with all its elements equal to 1, and $w(t)$ is the ground acceleration. With the notations indicated in Fig. 1, the matrices in equation (1) have the following structures:

$$\mathbf{M} = \begin{bmatrix} \mathbf{M_L} & \mathbf{0} \\ \mathbf{0} & \mathbf{M_R} \end{bmatrix},$$

$$\mathbf{M_L} = \text{diag}\left[m_1^{(l)}, m_2^{(l)}, m_3^{(l)}\right], \quad \mathbf{M_R} = \text{diag}\left[m_1^{(r)}, m_2^{(r)}\right],$$

$$\mathbf{C} = \mathbf{C^s} + \mathbf{C^d}, \qquad \mathbf{K} = \mathbf{K^s} + \mathbf{K^d}.$$

The inter-story damping matrix is

$$\mathbf{C^s} = \begin{bmatrix} \mathbf{C_L} & \mathbf{0} \\ \mathbf{0} & \mathbf{C_R} \end{bmatrix},$$

with

$$\mathbf{C_L} = \begin{bmatrix} c_1^{(l)}+c_2^{(l)} & -c_2^{(l)} & 0 \\ -c_2^{(l)} & c_2^{(l)}+c_3^{(l)} & -c_3^{(l)} \\ 0 & -c_3^{(l)} & c_3^{(l)} \end{bmatrix}, \ \mathbf{C_R} = \begin{bmatrix} c_1^{(r)}+c_2^{(r)} & -c_2^{(r)} \\ -c_2^{(r)} & c_2^{(r)} \end{bmatrix},$$

while the inter-building damping matrix corresponding to the viscoelastic dampers is

$$\mathbf{C^d} = \begin{bmatrix} c_1^{(d)} & 0 & 0 & -c_1^{(d)} & 0 \\ 0 & c_2^{(d)} & 0 & 0 & -c_2^{(d)} \\ 0 & 0 & 0 & 0 & 0 \\ -c_1^{(d)} & 0 & 0 & c_1^{(d)} & 0 \\ 0 & -c_2^{(d)} & 0 & 0 & c_2^{(d)} \end{bmatrix}.$$

Analogously, the inter-story stiffness matrix is

$$\mathbf{K^s} = \begin{bmatrix} \mathbf{K_L} & \mathbf{0} \\ \mathbf{0} & \mathbf{K_R} \end{bmatrix},$$

with

$$\mathbf{K_L} = \begin{bmatrix} k_1^{(l)}+k_2^{(l)} & -k_2^{(l)} & 0 \\ -k_2^{(l)} & k_2^{(l)}+k_3^{(l)} & -k_3^{(l)} \\ 0 & -k_3^{(l)} & k_3^{(l)} \end{bmatrix}, \ \mathbf{K_R} = \begin{bmatrix} k_1^{(r)}+k_2^{(r)} & -k_2^{(r)} \\ -k_2^{(r)} & k_2^{(r)} \end{bmatrix},$$

and the inter-building stiffness matrix takes the form

$$\mathbf{K^d} = \begin{bmatrix} k_1^{(d)} & 0 & 0 & -k_1^{(d)} & 0 \\ 0 & k_2^{(d)} & 0 & 0 & -k_2^{(d)} \\ 0 & 0 & 0 & 0 & 0 \\ -k_1^{(d)} & 0 & 0 & k_1^{(d)} & 0 \\ 0 & -k_2^{(d)} & 0 & 0 & k_2^{(d)} \end{bmatrix}.$$

From the second-order model (1), a first-order state-space model can be derived

$$\mathcal{S}: \begin{cases} \dot{x}(t) = Ax(t) + Bu(t) + Ew(t), \\ y(t) = C_y\, x(t). \end{cases} \tag{2}$$

Here, the state vector $x(t) \in \mathbb{R}^{10}$ groups together the displacements and the velocities arranged in increasing order, that is,

$$x(t) = [\, q_1(t), \dot{q}_1(t), \cdots, q_5(t), \dot{q}_5(t)]^T,$$

where $q_i(t) = q_i^{(l)}(t)$, $i$=1, 2, 3, is the displacement relative to the ground of the $i$th story in the left building, and $q_4(t)$=$q_1^{(r)}(t)$, $q_5(t)$=$q_2^{(r)}(t)$ denote the displacements for the right building. The matrices for the state-space model (2) used in the controllers design and the response numerical simulations are

$$A = \begin{bmatrix} 0 & 1 & 0 & 0 & 0 & 0 & 0 & 0 & 0 & 0 \\ -6201 & -0.2 & 3100 & 0.1 & 0 & 0 & 0 & 0 & 0 & 0 \\ 0 & 0 & 0 & 1 & 0 & 0 & 0 & 0 & 0 & 0 \\ 3100 & 0.1 & -6201 & -0.9 & 3100 & 0.1 & 0 & 0 & 0 & 0.8 \\ 0 & 0 & 0 & 0 & 0 & 1 & 0 & 0 & 0 & 0 \\ 0 & 0 & 3100 & 0.1 & -3100 & -0.1 & 0 & 0 & 0 & 0 \\ 0 & 0 & 0 & 0 & 0 & 0 & 0 & 1 & 0 & 0 \\ 0 & 0 & 0 & 0 & 0 & 0 & -3100 & -0.2 & 1550 & 0.1 \\ 0 & 0 & 0 & 0 & 0 & 0 & 0 & 0 & 0 & 1 \\ 0 & 0 & 0 & 0.8 & 0 & 0 & 1550 & 0.1 & -1550 & -0.9 \end{bmatrix}$$

$$B = 10^{-6} \times \begin{bmatrix} 0 & 0 & 0 & 0 & 0 \\ 0.7752 & 0 & 0 & 0 & 0 \\ 0 & 0 & 0 & 0 & 0 \\ 0 & 0.7752 & 0 & 0 & 0 \\ 0 & 0 & 0 & 0 & 0 \\ 0 & 0 & 0.7752 & 0 & 0 \\ 0 & 0 & 0 & 0 & 0 \\ 0 & 0 & 0 & 0.7752 & 0 \\ 0 & 0 & 0 & 0 & 0 \\ 0 & 0 & 0 & 0 & 0.7752 \end{bmatrix},$$

$$E = [\, 0, -1, 0, -1, 0, -1, 0, -1, 0, -1]^T,$$

$$C_y = \begin{bmatrix} 1 & 0 & 0 & 0 & 0 & 0 & 0 & 0 & 0 & 0 \\ -1 & 0 & 1 & 0 & 0 & 0 & 0 & 0 & 0 & 0 \\ 0 & 0 & -1 & 0 & 1 & 0 & 0 & 0 & 0 & 0 \\ 0 & 0 & 0 & 0 & 0 & 0 & 1 & 0 & 0 & 0 \\ 0 & 0 & 0 & 0 & 0 & 0 & -1 & 0 & 1 & 0 \end{bmatrix}. \tag{3}$$

It should be noted that the output matrix $C_y$ extracts the inter-story drifts of the buildings, that is,

$$y(t) = \left[y_1^{(l)}(t), y_2^{(l)}(t), y_3^{(l)}(t), y_1^{(r)}(t), y_2^{(r)}(t)\right]^T,$$

where $y_1^{(l)}$=$q_1^{(l)}$, $y_2^{(l)}$=$q_2^{(l)} - q_1^{(l)}$, $y_3^{(l)}$=$q_3^{(l)} - q_2^{(l)}$, $y_1^{(r)}$=$q_1^{(r)}$, $y_2^{(r)}$=$q_2^{(r)} - q_1^{(r)}$. The matrices in (3) correspond to the following particular values of the mass, damping and stiffness coefficients: $m_i^{(l)}$=$m_j^{(r)}$=1.29×10$^6$ Kg; $c_i^{(l)}$=$c_j^{(r)}$=10$^5$ N s/m; $k_i^{(l)}$=4×10$^9$N/m; $k_j^{(r)}$=2×10$^9$N/m; $c_1^{(d)}$=0, $c_2^{(d)}$=10$^6$ N s/m; $k_j^{(d)}$=0, for $i$=1, 2, 3, $j$=1, 2. A detailed derivation of the first-order state-space model (2) can be found in Wang et al. (2009).

## 3. CONTROLLERS DESIGN

In this section, three active $H_\infty$ controllers for the system (2) are computed: a centralized controller and two decentralized controllers; in all the cases, the particular values given in (3) are used. The centralized controller will be taken as a reference in the performance assessment. For the decentralized controllers, two different approaches are followed: a centralized design which uses the overall two-building coupled model, and a decentralized design which considers the buildings independently, ignoring the linkage. Regarding to the passive control system, the buildings are linked by a single damper with damping constant $c_2^{(d)}$=10$^6$ N s/m, located at the second story. This configuration may be considered as optimal, in the sense that numerical simulations show that no significant reduction of the vibrational response results when a similar damper is placed linking the first stories, or elastic linking elements are considered. In terms of the damping and stiffness coefficients, this means $c_1^{(d)}$=0, $k_1^{(d)}$=$k_2^{(d)}$=0. Finally, a number of good reasons justify the choice of the $H_\infty$ approach for the problem under consideration: the practical interpretation of the $H_\infty$ norm as minimum worst case gain from energy disturbance to energy response, the existence of efficient solvers via LMI formulation which allow to obtain decentralized controllers by imposing structure constraints on the controller gain matrix, and the possibility of extending the study to a variety of interesting scenarios which

may include several kinds of uncertainties, delays, actuator saturation, etc.

### *3.1 $H_\infty$ control*

In this subsection, a brief summary of $H_\infty$ control design is presented; a detailed treatment can be found in Boyd et al. (1994). Let us consider the system (2) together with the controlled output $z(t)$=$C_z x(t)$+$D_z u(t)$ where $C_z$ and $D_z$ are, respectively, the state and control-force controlled output matrices. For a given state feedback controller $u(t)$=$Gx(t)$, the following closed-loop system results

$$\mathcal{S}_{CL}: \begin{cases} \dot{x}(t) &= A_{CL}x(t) + Ew(t), \\ z(t) &= C_{CL}x(t), \end{cases} \tag{4}$$

where

$$A_{CL} = A + BG, \quad C_{CL} = C_z + D_z G. \tag{5}$$

The closed-loop transfer function from the disturbance $w(t)$ to the controlled output $z(t)$ has the form

$$T_{zw}(s) = C_{CL}\left(sI - A_{CL}\right)^{-1} E. \tag{6}$$

The objective is to find a gain matrix $G_{op}$ which produces a stable matrix $A_{CL}$ and, at the same time, minimizes the value of the norm

$$\|T_{zw}\|_\infty = \max_\omega \ \bar{\sigma}\left[T_{zw}(j\omega)\right], \tag{7}$$

where $\bar{\sigma}(\cdot)$ denotes the maximum singular value. For a prescribed $\gamma$>0, according to the Bounded Real Lemma, the following two statements are equivalent:

(1) $\|T_{zw}\|_\infty$<$\gamma$ and $A_{CL}$ is stable.

(2) There exists a symmetric positive-definite matrix $P\in\mathbb{R}^{2n\times 2n}$ such that the following inequality

$$\begin{bmatrix} A_{CL}P+PA_{CL}^T+\gamma^{-2}EE^T & PC_{CL}^T \\ * & -I \end{bmatrix} < 0 \tag{8}$$

holds, where $*$ denotes the symmetric entry.

By using the closed-loop matrix definitions given in (5), equation (8) becomes

$$\begin{bmatrix} AP+PA^T+BGP+PG^TB^T+\gamma^{-2}EE^T & PC_z^T+PG^TD_z^T \\ * & -I \end{bmatrix} < 0.$$

The above nonlinear matrix inequality can be converted into a linear matrix inequality (LMI) by introducing the new variables $Y$=$GP$ and $\eta$=$\gamma^{-2}$

$$\begin{bmatrix} AP+PA^T+BY+Y^TB^T+\eta EE^T & PC_z^T+Y^TD_z^T \\ * & -I \end{bmatrix} < 0. \tag{9}$$

The continuous-time $H_\infty$ control problem is then transformed into the following convex optimization problem:

$$\begin{cases} \text{maximize } \eta \\ \text{subject to } P>0,\ \eta>0 \text{ and the LMI (9)}, \end{cases} \tag{10}$$

where the matrices $Y$, $P$ are the optimization variables. If the optimal value $\eta_{\max}$ is attained for the optimal matrices $Y_{op}$, $P_{op}$, the corresponding gain matrix can be computed as

$$G_{op} = Y_{op}\,P_{op}^{-1}, \tag{11}$$

and the value of the minimum $H_\infty$ norm is

$$\|T_{zw}(G_{op})\|_\infty = \gamma_{G_{op}} = \frac{1}{\sqrt{\eta_{\max}}}, \tag{12}$$

where $T_{zw}(G_{op})$ denotes the transfer function described in (6) corresponding to the control gain matrix $G_{op}$.

### *3.2 Centralized Control*

First, we compute a centralized $H_\infty$ control by solving the optimization problem stated in (10) using the system matrices given in (3) and the controlled output matrices

$$C_z = \begin{bmatrix} C_y \\ \mathbf{0}_{5\times 10} \end{bmatrix}, \quad D_z = 0.3162\times 10^{-7}\begin{bmatrix} \mathbf{0}_{5\times 5} \\ \mathbf{I}_{5\times 5} \end{bmatrix},$$

obtaining the following full control gain matrix

$G_c = 10^7\times$
$$\begin{bmatrix} 0.133 & -0.061 & 0.180 & -0.082 & 0.289 & -0.083 & -0.810 & -0.031 & -1.422 & -0.050 \\ 0.275 & -0.082 & 0.344 & -0.145 & 0.498 & -0.165 & -1.515 & -0.055 & -2.527 & -0.091 \\ 0.302 & -0.083 & 0.470 & -0.165 & 0.594 & -0.226 & -1.992 & -0.070 & -3.071 & -0.113 \\ 0.711 & -0.031 & 1.300 & -0.057 & 1.687 & -0.070 & -0.254 & -0.072 & -0.445 & -0.067 \\ 1.231 & -0.050 & 2.227 & -0.091 & 2.573 & -0.113 & -0.336 & -0.067 & -0.736 & -0.138 \end{bmatrix}$$

and the minimum $\gamma$ value

$$\left\|T_{zw(G_c)}\right\|_\infty = \gamma_{G_c} = 0.0788.$$

Note that to compute the actuation force for any story using the gain matrix $G_c$, the knowledge of the complete state of both buildings is required.

### *3.3 Decentralized Control with Centralized Design*

Second, we consider again the overall two-building coupled system but now the goal is to design a decentralized controller by imposing a block diagonal structure on the control gain matrix. To this end, we solve problem (10) using variable matrices $P$ and $Y$ with the form

$$P = \begin{bmatrix} P_{11} & 0 \\ 0 & P_{22} \end{bmatrix}, \quad Y = \begin{bmatrix} Y_{11} & 0 \\ 0 & Y_{22} \end{bmatrix},$$

where $P_{11}$, $P_{22}$ are positive-definite matrices of dimensions $6\times 6$ and $4\times 4$, respectively, and $Y_{11}$, $Y_{22}$ are rectangular matrices of dimensions $3\times 6$ and $2\times 4$. The matrices used in the controlled output $z(t)$=$C_z x(t)$+$D_z u(t)$ are

$$C_z = \begin{bmatrix} C_y \\ \mathbf{0}_{5\times 10} \end{bmatrix}, \quad D_z = 0.5623\times 10^{-7}\begin{bmatrix} \mathbf{0}_{5\times 5} \\ \mathbf{I}_{5\times 5} \end{bmatrix}.$$

After solving the corresponding constrained LMI minimization problem, the following block diagonal gain matrix results

$G_{dc} = 10^6\times$
$$\begin{bmatrix} 0.078 & -1.049 & 0.094 & -1.177 & -0.230 & -1.426 & 0 & 0 & 0 & 0 \\ 0.320 & -1.177 & 0.056 & -2.476 & -0.268 & -2.603 & 0 & 0 & 0 & 0 \\ 0.497 & -1.426 & 0.190 & -2.603 & -0.346 & -3.653 & 0 & 0 & 0 & 0 \\ 0 & 0 & 0 & 0 & 0 & 0 & 0.057 & -1.220 & -0.153 & -1.346 \\ 0 & 0 & 0 & 0 & 0 & 0 & 0.354 & -1.346 & -0.269 & -2.566 \end{bmatrix}$$

and the associated minimum $\gamma$ value is

$$\|T_{zw}(G_{dc})\|_\infty = \gamma_{G_{dc}} = 0.1544.$$

In this case, we only need the state of the corresponding building to compute the actuation force for a given story. Predictably, a higher $\gamma$ value has been obtained due to the structural restrictions imposed on matrices $Y$ and $P$; however, the resulting $\gamma$ value is still remarkably low.

### *3.4 Decentralized Control with Decentralized Design*

Finally, we proceed to design a decentralized controller considering the buildings independently and ignoring the passive linking system. In this third case, we have two independent subsystems

$$\mathcal{S}_L: \begin{cases} \dot{x}_L(t) = A_L\,x_L(t) + B_L\,u_L(t) + E_L\,w(t), \\ y_L(t) = (C_y)_L\,x_L(t), \end{cases} \tag{13}$$

$$\mathcal{S}_R : \begin{cases} \dot{x}_R(t) = A_R x_R(t) + B_R u_R(t) + E_R w(t), \\ y_R(t) = (C_y)_R\, x_R(t), \end{cases} \tag{14}$$

with state vectors

$$x_L(t) = \left[ q_1^{(l)}(t), \dot{q}_1^{(l)}(t),\, q_2^{(l)}(t), \dot{q}_2^{(l)}(t),\, q_3^{(l)}(t), \dot{q}_3^{(l)}(t) \right]^T,$$

$$x_R(t) = \left[ q_1^{(r)}(t), \dot{q}_1^{(r)}(t),\, q_2^{(r)}(t), \dot{q}_2^{(r)}(t) \right]^T,$$

control forces

$$u_L(t) = \left[ u_1^{(l)}(t), u_2^{(l)}(t), u_3^{(l)}(t) \right]^T, \quad u_R(t) = \left[ u_1^{(r)}(t), u_2^{(r)}(t) \right]^T,$$

and outputs

$$y_L(t) = \left[ y_1^{(l)}(t), y_2^{(l)}(t), y_3^{(l)}(t) \right]^T, \quad y_R(t) = \left[ y_1^{(r)}(t), y_2^{(r)}(t) \right]^T.$$

The matrices in (13) and (14) can be easily derived from the matrices and values given in Section 2; for instance, the output matrices are

$$(C_y)_L = \begin{bmatrix} 1 & 0 & 0 & 0 & 0 & 0 \\ -1 & 0 & 1 & 0 & 0 & 0 \\ 0 & 0 & -1 & 0 & 1 & 0 \end{bmatrix}, \quad (C_y)_R = \begin{bmatrix} 1 & 0 & 0 & 0 \\ -1 & 0 & 1 & 0 \end{bmatrix}.$$

For the left subsystem $\mathcal{S}_L$, we consider the controlled output

$$z_L(t) = (C_z)_L x_L(t) + (D_z)_L u_L(t)$$

with

$$(C_z)_L = \begin{bmatrix} (C_y)_L \\ \mathbf{0}_{3\times 6} \end{bmatrix}, \quad (D_z)_L = 0.5623 \times 10^{-7} \begin{bmatrix} \mathbf{0}_{3\times 3} \\ \mathbf{I}_{3\times 3} \end{bmatrix},$$

to compute an $H_\infty$ controller $G_L$. Analogously, for the right subsystem $\mathcal{S}_L$ we take

$$z_R(t) = (C_z)_R x_R(t) + (D_z)_R u_R(t),$$

$$(C_z)_R = \begin{bmatrix} (C_y)_R \\ \mathbf{0}_{2\times 4} \end{bmatrix}, \quad (D_z)_R = 0.5623 \times 10^{-7} \begin{bmatrix} \mathbf{0}_{2\times 2} \\ \mathbf{I}_{2\times 2} \end{bmatrix},$$

to independently compute the gain matrix $G_R$. Arranging $G_L$ and $G_R$ in a block diagonal gain matrix, the following decentralized controller results

$$G_{dd} = 10^6 \times \begin{bmatrix} 0.050 & -0.774 & -0.003 & -0.953 & -0.096 & -1.095 & 0 & 0 & 0 & 0 \\ 0.212 & -0.953 & -0.019 & -1.868 & -0.133 & -2.048 & 0 & 0 & 0 & 0 \\ 0.279 & -1.095 & 0.074 & -2.048 & -0.190 & -2.822 & 0 & 0 & 0 & 0 \\ 0 & 0 & 0 & 0 & 0 & 0 & 0.097 & -1.905 & -0.188 & -2.421 \\ 0 & 0 & 0 & 0 & 0 & 0 & 0.418 & -2.421 & -0.298 & -4.326 \end{bmatrix}$$

In this case, the minimum $\gamma$ value is not available; however, the $H_\infty$ norm can be directly computed using (5)–(7), resulting

$$\|T_{zw}(G_{dd})\|_\infty = 0.1550.$$

In Fig. 2, the maximum singular value curves of the transfer functions $T_{zw}(G_c)$, $T_{zw}(G_{dc})$, and $T_{zw}(G_{dd})$ are displayed. Note that the curves corresponding to the decentralized controllers $G_{dc}$ and $G_{dd}$ are practically coincident.

## 4. NUMERICAL SIMULATIONS

In this section, numerical simulations of the free and controlled responses of the two-building system, using the El Centro 1940 earthquake as acceleration input, are presented. The maximum absolute inter-story drifts, and the maximum absolute control forces for the left and right building are displayed in Fig. 3 and Fig. 4, respectively. Five cases of response are showed: (i) free response of the uncoupled system (denoted by Free in the legend), no passive or active control devices are working in this case; (ii) free response of the coupled system, i.e. response

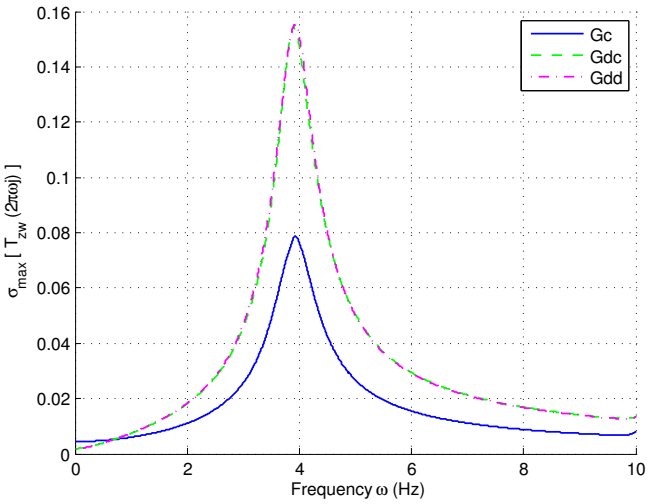


Figure 2. Maximum singular values.

under passive control (denoted by Passive); (iii) response of the coupled system under the centralized active control (denoted by $G_c$); (iv) response of the coupled system under the decentralized active controller with centralized design (denoted by $G_{dc}$); and (v) response of the coupled system under the decentralized active controller with decentralized design (denoted by $G_{dd}$).

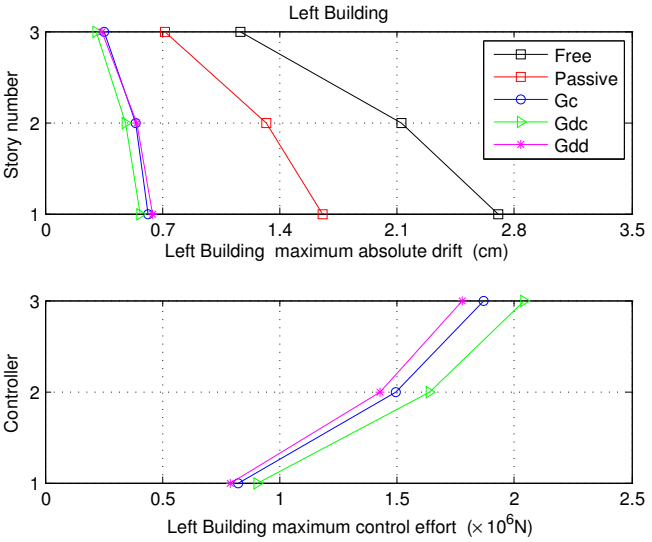


Figure 3. Left building inter-story drifts and control forces

The graphics show that a remarkable reduction of the vibrational response is achieved by the passive control system. Regarding the active controllers, the performance of the decentralized controllers $G_{dc}$ and $G_{dd}$ is certainly excellent: both controllers behave practically the same as the overall centralized controller, in some cases with a slightly higher control effort.

Next, we consider the partial and full failure of the active decentralized controller $G_{dd}$. Table 1 presents the maximum inter-story drifts for full failure (Passive) and two cases of partial failure (Left failure, Right failure). The corresponding maximum absolute control actions are collected in Table 2. As a reference, these tables also include the data for the free response, actively controlled

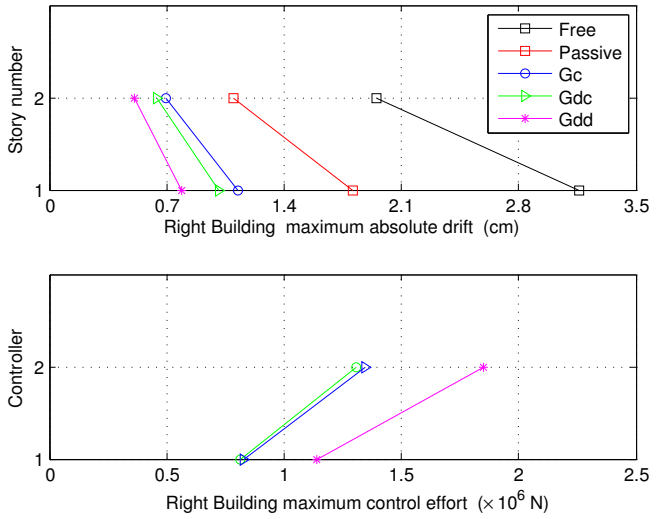


Figure 4.Right building inter-story drifts and control forces

response with the centralized controller $G_c$, and non-failure response with the decentralized controller $G_{dd}$.

| | Left Building | | | Right Building | |
|---|---|---|---|---|---|
| | $y_1^{(l)}$ | $y_2^{(l)}$ | $y_3^{(l)}$ | $y_1^{(r)}$ | $y_2^{(r)}$ |
| Free | 2.71 | 2.13 | 1.17 | 3.16 | 1.95 |
| Passive | 1.65 | 1.32 | 0.72 | 1.81 | 1.10 |
| Centralized ($G_c$) | 0.62 | 0.54 | 0.35 | 1.13 | 0.70 |
| Decentralized ($G_{dd}$) | 0.64 | 0.54 | 0.34 | 0.79 | 0.51 |
| Left failure | 1.24 | 1.04 | 0.61 | 0.83 | 0.53 |
| Right failure | 0.67 | 0.57 | 0.35 | 1.65 | 1.03 |

Table 1. Max. absolute inter-story drifts (cm)

In case of a full failure of the active control system, a remarkable reduction of the maximum inter-story drifts in both buildings is achieved by the passive element. When one of the local active controllers fails, the building that remains actively controlled is not affected by the failure. Moreover, the control forces in the working active controller increase slightly and act through the linking element to drive the response of the failing building to a level that is clearly below the level obtained by the pure passive control. In all the cases, the results achieved by the decentralized controller $G_{dd}$ are similar to those obtained by the centralized control.

| | Left Building | | | Right Building | |
|---|---|---|---|---|---|
| | $u_1^{(l)}$ | $u_2^{(l)}$ | $u_3^{(l)}$ | $u_1^{(r)}$ | $u_2^{(r)}$ |
| Centralized ($G_c$) | 0.82 | 1.49 | 1.87 | 0.81 | 1.31 |
| Decentralized ($G_{dd}$) | 0.79 | 1.43 | 1.78 | 1.14 | 1.85 |
| Left failure | 0 | 0 | 0 | 1.19 | 1.93 |
| Right failure | 0.82 | 1.47 | 1.84 | 0 | 0 |

Table 2. Max. abs. actuation force ($\times 10^6$N)

The obtained results can also be seen from another interesting perspective. Buildings containing all sort of delicate equipment such as laboratories, operating rooms, large computer servers, telecommunication machinery, etc., may require a higher seismic protection than building containing more ordinary facilities as offices or meeting rooms. In this context, the four working states of the active decentralized controller: full working, left disabled, right disabled, and full disabled, can be understood as different control configurations corresponding to different levels of seismic protection. Thus, for two adjacent buildings which require a normal seismic protection, a passive link may be a good option; in the case that just one of the buildings needs special seismic protection, the data in Tables 1 and 2 suggest that the implementation of an active controller in this building together with a passive link may be an excellent option to obtain a proper level of seismic protection in both buildings. Moreover, the passive linking will help to mitigate pounding effects, and may also guarantee a remarkable level of seismic protection if the active control fails.

## 5. CONCLUSIONS

A passive-active structural vibration control for adjacent buildings consisting in a combination of passive linking elements with an active decentralized $H_\infty$ control system has been designed. Numerical simulations show that the overall active-passive control system achieves excellent results when the active control system works; in case of full or partial failure of the active control system, a remarkable reduction in the vibrational response is guaranteed by the passive linking elements. The results also indicate that the implementation of an active control system in just one of the buildings together with a passive link may be a good control strategy for adjacent buildings which require different levels of seismic protection.

## REFERENCES

Anagnostopoulos, S. (1996). Building pounding re-examined: How serious a problem is it? In *Eleventh World Conference of Earthquake Engineering*, Paper No 2108. Elsevier Science ltd.

Bharti, S., Dumne, S., and Shrimali, M. (2010). Seismic response analysis of adjacent buildings connected with magnetorheological dampers. *Engineering Structures*, (32), 2122–2133.

Boyd, S., Ghaoui, L.E., Feron, E., and Balakrishnan, V. (1994). *Linear Matrix Inequalities in System and Control Theory*. SIAM Studies in Applied Mathematics, Philadelphia, USA.

Housner, G., Bergman, L., Caughey, T., and Chassiakos, A. (1997). Structural control: Past, present, and future. *Journal of Engineering Mechanics*, 123(9), 897–971.

Lopez-Garcia, D. and Soong, T. (2009). Assessment of the separation necessay to prevent seismic pounding between structural systems. *Probabilistic Engineering Mechanics*, (24), 210–223.

Matsagar, V. and Jangid, R. (2005). Viscoelastic damper connected to adjacent structures involving seismic isolation. *Journal of Civil Engineering and Management*, XI(4), 309–322.

Preumont, A. and Seto, K. (2008). *Active Control of Structures*. Wiley, United Kingdom.

Spencer, B. and Nagarajaiah, S. (2003). State of the art of structrual control. *Journal of Structural Engineering*, 129(7), 845–856.

Wang, Y., Lynch, J., and Law, K. (2009). Decentralized $H_\infty$ controller design for large-scale civil structures. *Earthquake Engineering and Structural Dynamics*, 38, 377–401.